BIOCHEMISTRY
including biophysical chemistry & molecular biology

ARTICLE

pubs.acs.org/biochemistry

Conformational Folding and Stability of the HET-C2 Glycolipid Transfer Protein Fold: Does a Molten Globule-like State Regulate Activity?

Roopa Kenoth,[†,¶] Ravi Kanth Kamlekar,[†,¶] Dhirendra K. Simanshu,[‡,¶] Yongguang Gao,[†] Lucy Malinina,[§] Franklyn G. Prendergast,[∥] Julian G. Molotkovsky,[⊥] Dinshaw J. Patel,[*,‡] Sergei Y. Venyaminov,[*,∥] and Rhoderick E. Brown[*,†]

[†]The Hormel Institute, University of Minnesota, Austin, Minnesota 55912, United States

[‡]Structural Biology Program, Memorial Sloan-Kettering Cancer Center, New York, New York 10065, United States

[§]Structural Biology, CIC bioGUNE, Derio, Spain

[∥]Mayo Clinic College of Medicine, Rochester, Minnesota 55905, United States

[⊥]Shemyakin and Ovchinnikov Institute of Bioorganic Chemistry, Russian Academy of Sciences, Moscow, Russia

Supporting Information

ABSTRACT: The glycolipid transfer protein (GLTP) superfamily is defined by the human GLTP fold that represents a novel motif for lipid binding and transfer and for reversible interaction with membranes, i.e., peripheral amphitropic proteins. Despite limited sequence homology with human GLTP, we recently showed that HET-C2 GLTP of *Podospora anserina* is organized conformationally as a GLTP fold. Currently, insights into the folding stability and conformational states that regulate GLTP fold activity are almost nonexistent. To gain such insights into the disulfide-less GLTP fold, we investigated the effect of a change in pH on the fungal HET-C2 GLTP fold by taking advantage of its two tryptophans and four tyrosines (compared to three tryptophans and 10 tyrosines in human GLTP). pH-induced conformational alterations were determined by changes in (i) intrinsic tryptophan fluorescence (intensity, emission wavelength maximum, and anisotropy), (ii) circular dichroism over the near-UV and far-UV ranges, including thermal stability profiles of the derivatized molar ellipticity at 222 nm, (iii) fluorescence properties of 1-anilinonaphthalene-8-sulfonic acid, and (iv) glycolipid intermembrane transfer activity monitored by Förster resonance energy transfer. Analyses of our recently determined crystallographic structure of HET-C2 (1.9 Å) allowed identification of side chain electrostatic interactions that contribute to HET-C2 GLTP fold stability and can be altered by a change in pH. Side chain interactions include numerous salt bridges and interchain cation−π interactions, but not intramolecular disulfide bridges. Histidine residues are especially important for stabilizing the local positioning of the two tryptophan residues and the conformation of adjacent chains. Induction of a low-pH-induced, molten globule-like state inhibited glycolipid intermembrane transfer by the HET-C2 GLTP fold.

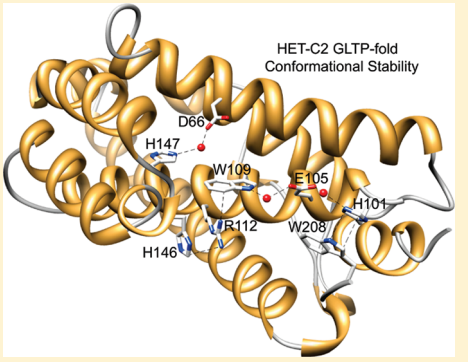

Characterization of protein stability and folding intermediates can provide insights into normal folding mechanisms as well as pathological conditions involving protein aggregation (e.g., Alzheimer's disease). A partially unfolded state of special interest is the molten globule (MG) state, which maintains a compact organization with pronounced secondary structure but lacks a tertiary conformation.[1−4] MG-like states have been linked to a number of biological processes such as protein−protein interactions and protein insertion and translocation into membranes, including the action of lipid binding/transfer proteins.[5−12]

In filamentous fungi, *Het* genes play a major role in vegetative incompatibility processes involving cell−cell recognition.[13−16] One *Het* gene product, HET-C2, is known to act as a lipid binding/transfer protein that is specific for simple glycosphingolipids.[17,18] Recently, we showed that HET-C2 is organized as a two-layer "sandwich" dominated by α-helices[18] and is folded in a manner very similar to that of human glycolipid transfer protein (GLTP), which serves as the prototype and founding member of the GLTP superfamily.[19−21] Like human GLTP,[22] HET-C2 acquires and delivers glycolipids by interacting transiently and reversibly with membranes.[17,18] Thus, HET-C2 displays the defining features of a peripheral amphitropic membrane protein, which typically has affinity for both aqueous and nonpolar environments but requires

Received: March 15, 2011
Revised: May 6, 2011
Published: May 10, 2011

neither post-translational modifications nor anchor proteins for reversible interaction with membranes.[23,24]

At present, very limited information about the stability of the GLTP fold and the physical conditions that can affect folding status is available. Moreover, it is not known whether partially unfolded (e.g., MG-like states) play any role in GLTP fold functionality. What is known is that human GLTP has a highly cooperative unfolding transition that occurs near 54 °C at neutral pH,[25] consistent with the 55 °C inactivation reported by Nylund and Mattjus.[26] However, HET-C2 exhibits a 4−5 °C lower unfolding transition temperature midpoint (∼49 °C) at neutral pH despite being a GLTP fold.[18] Further characterization under various physical conditions is likely to provide an improved understanding of the key parameters controlling GLTP fold stability and folding. Our strategy was to take advantage of the simpler Trp and Tyr composition of HET-C2 (two Trp and four Tyr residues) compared to that of GLTP (three Trp and 10 Tyr residues) and to use fluorescence and far-UV and near-UV circular dichroism (CD) spectroscopy to further elucidate the relationship between GLTP fold conformation and functionality. Herein, we have characterized the pH dependence of HET-C2 stability and activity as well as investigated whether partially unfolded, pH-induced, MG-like states regulate the glycolipid transfer activity of HET-C2.

EXPERIMENTAL PROCEDURES

Expression and Purification of HET-C2. HET-C2 was expressed and purified in a manner similar to that of GLTP[18,27] using pET-30 Xa/LIC (Novagen) containing *het-c2* ORF of *Podospora anserina* (GenBank entry U05236). Transformed BL21 cells (*Escherichia coli*) grown at 37 °C overnight in Luria-Bertani medium were induced with IPTG (0.1 mM) and then grown for 16−20 h at 15 °C. Purification of rHET-C2 from soluble lysate protein was accomplished by Ni-NTA affinity chromatography. The N-terminal His-S tag was removed using factor Xa, yielding a protein identical in sequence to native HET-C2. HET-C2 was repurified by fast protein liquid chromatography size exclusion chromatography using a HiLoad 16/60 Superdex-75 prep grade column (Amersham). HET-C2 fractions were pooled, concentrated centrifugally (10 kDa cutoff membrane), and checked for purity by sodium dodecyl sulfate−polyacrylamide gel electrophoresis.

Fluorescence Measurements. The Trp fluorescence of HET-C2 was measured at 25 °C from 310 to 420 nm with a SPEX Fluoromax spectrofluorimeter (Horiba Scientific, Edison, NJ) using excitation and emission bandpasses of 5 nm. Excitation at 295 nm minimized contributions from Tyr, and the protein concentration was kept at an OD_{295} to <0.1 to avoid inner filter effects.[25,28,29] Fluorescence polarization measurements of Trp were performed at room temperature (25 °C) using a Hitachi polarization accessory. Anisotropy values were calculated using eq 1:

$$r = (I_{VV} - GI_{VH})/(I_{VV} + 2GI_{VH}) \quad (1)$$

where I_{VV} and I_{VH} are the background-subtracted, measured fluorescence intensities obtained with the excitation polarizer vertically oriented and the emission polarizer vertically and horizontally oriented, respectively. The grating correction factor (G) is the efficiency ratio of the detection system for vertically and horizontally polarized light and equals I_{VH}/I_{HH}. For measurements of 1-anilinonaphthalene-8-sulfonic acid (ANS), excitation occurred at 375 nm and the emission intensity was recorded from 400 to 560 nm.

Circular Dichroism Spectroscopy. CD spectra were recorded using a J-810 spectropolarimeter (JASCO) equipped with a CTC-345 temperature-control system at 50 μM HET-C2 and 10 °C in 10 mM sodium bicarbonate (pH 10), carbonate-bicarbonate (pH 8 or 9), phosphate (pH 6 or 7.4), citrate-phosphate (pH 3, 4, or 5), or glycine-HCl (pH 2) being purged continuously with N_2. Spectral and temperature dependence measurements in the far-UV (185−250 nm) and near-UV (250−320 nm) ranges were performed as detailed previously (refs 18 and 25 and references therein). Also detailed are calculations of HET-C2 secondary structure from far-UV CD spectra using CDPro and of tertiary structure class using CDPro CLUSTER.

Protein Concentration. The concentration of HET-C2 (molar absorptivity at 280 nm of 17.12 mM^{-1} cm^{-1}) was measured using a Beckman DU 640 spectrophotometer at a 1.8 nm bandwidth and averaging results from four calculation methods.[30−33] Spectra were corrected for turbidity by plotting the log dependence of solution absorbance versus the log of the wavelength and extrapolating their linear dependence in the 320−440 nm range to the 240−320 nm absorption range using the DU-640 scatter correction routine. Extrapolated absorbance values were subtracted from measured values, decreasing the apparent protein absorbance at ∼280 nm by ∼15%.

HET-C2 Transfer Activity of Glycolipid. Continuous real-time monitoring of glycolipid intermembrane transfer by HET-C2 and determination of initial lipid transfer rates were conducted by Förster resonance energy transfer (FRET) using a continuously stirred sample (∼100 rpm) maintained at 25 ± 0.1 °C (Neslab, RTE-111) while measuring emission intensity at 425 nm.[17] Both fluorescent lipids {1 mol % AV-glycolipid containing the anthrylvinyl fluorophore at the ω-acyl position [(11*E*)-12-(9-anthryl)-11-dodecenoyl acyl chain] and 1.5 mol % 1-acyl-2-[9-(3-perylenoyl)nonanoyl]-*sn*-glycero-3-phosphocholine} (Per-PC) were initially localized in the donor vesicles comprised of POPC matrix and formed by rapid ethanol injection. Minimal emission by AV-glycolipid occurs upon excitation (370 nm) because of resonance energy transfer to nearby Per-PC. A minimal emission change also is elicited by the addition of pure sonicated POPC acceptor vesicles (10-fold excess) because of the slow time course of spontaneous lipid transfer. Addition of catalytic HET-C2 amounts causes a sudden, exponential increase in AV emission intensity (425 nm) as the protein extracts AV-labeled glycolipid from donor vesicles and delivers it to the acceptors (creating separation from the "non-transferable" perylenoyl lipid). Addition of Tween 20 detergent at the end of the kinetic time course provides a measure of maximal AV intensity that can be achieved by "infinite" separation from the perylenoyl fluorophore. The initial lipid transfer rate (v_o) is obtained by nonlinear regression analysis and fitting to first-order exponential behavior using ORIGIN 7.0 (Origin Lab, Northampton, MA). ΔF represents the AV emission intensity difference after extended incubation with HET-C2 compared to time zero with no HET-C2. The standard deviations in fitting are calculated at 95% confidence intervals, and R^2 values are >0.96 for all estimates.

RESULTS

Our recent determination of the HET-C2 structure by X-ray diffraction (1.9 Å) shows the global architecture to be

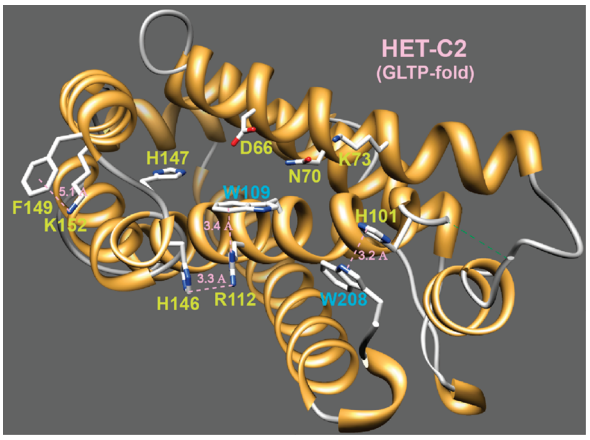

Figure 1. HET-C2 architecture. A GLTP fold has been determined for HET-C2 (Protein Data Bank entry 3kv0) by X-ray diffraction (1.9 Å).[18] Also depicted are the locations of Trp^{109} and Trp^{208} along with nearby residues (Arg^{112}, His^{146}, and His^{101}) that affect their topology.

a GLTP fold.[18] However, unlike human GLTP, which has three Trp residues,[19,28,34] HET-C2 contains only two Trp residues. As illustrated in Figure 1 and Figure S1 of the Supporting Information, Trp^{109} of α-helix 4 acts as a stacking plate in the glycolipid headgroup recognition center and helps orient the ceramide-linked sugar for hydrogen bonding with Asp^{66}, Asn^{70}, and Lys^{73}, thus functioning like Trp^{96} of human GLTP. Figure 1 also shows how Arg^{112} stabilizes the orientation of the Trp^{109} indole ring from beneath by cation−π interaction (~3.4 Å).[35] The orientation of the planar guanidinium moiety of Arg^{112} also is influenced by stacking (~3.3 Å) against the imidazole ring of His^{146} (α5−α6 loop).[36] The other Trp residue (Trp^{208}) forms the C-terminus of HET-C2, is surface accessible, and stacks (~3.2 Å) against the imidazole ring of His^{101} on the α3−α4 loop, thus distinguishing it from Trp^{85} and Trp^{142} of human GLTP. Because of the apparent involvement of the intrinsically fluorescent Trp^{109} and Trp^{208} residues in stabilizing HET-C2 architecture via their interactions with His^{146} and His^{101}, pH-induced conformational changes in HET-C2 were initially investigated using fluorescence spectroscopy.

pH Dependence of Trp Fluorescence in HET-C2. As shown in Figure 2A, the intrinsic Trp fluorescence of HET-C2 has an emission wavelength maximum (λ_{max}) that is strongly red-shifted (~354 nm at neutral pH), consistent with a highly polar environment for the fluorophore and in agreement with X-ray data showing surface localizations for the indole rings of Trp^{109} and Trp^{208} (Figure S2 of the Supporting Information). The HET-C2 Trp emission intensity is relatively high at and above neutral pH with the maximal intensity occurring near pH 10. Below neutral pH, Trp emission intensity decreases dramatically. This response contrasts that of λ_{max} (Figure 2B), which remains constant (~354 nm) over the pH 5.5−7 range but displays discernible λ_{max} blue shifts to ~353 nm at pH 5, 8, and 9 as well as to ~352 nm at pH 4 and 10. More pronounced λ_{max} blue shifts to ~349 nm occur at pH 2 and 3. The blue-shifted λ_{max} suggests a pH-induced conformational change that results in decreased polarity of the Trp average environment. For further evaluation, the anisotropy of the Trp emission signal was measured (Figure 2C). The overall pattern of pH-induced anisotropy change correlated remarkably well with that of the λ_{max} blue shifts. For instance, the Trp anisotropy was maximal and unaltered between pH 5.5 and 7. Moderate decreases

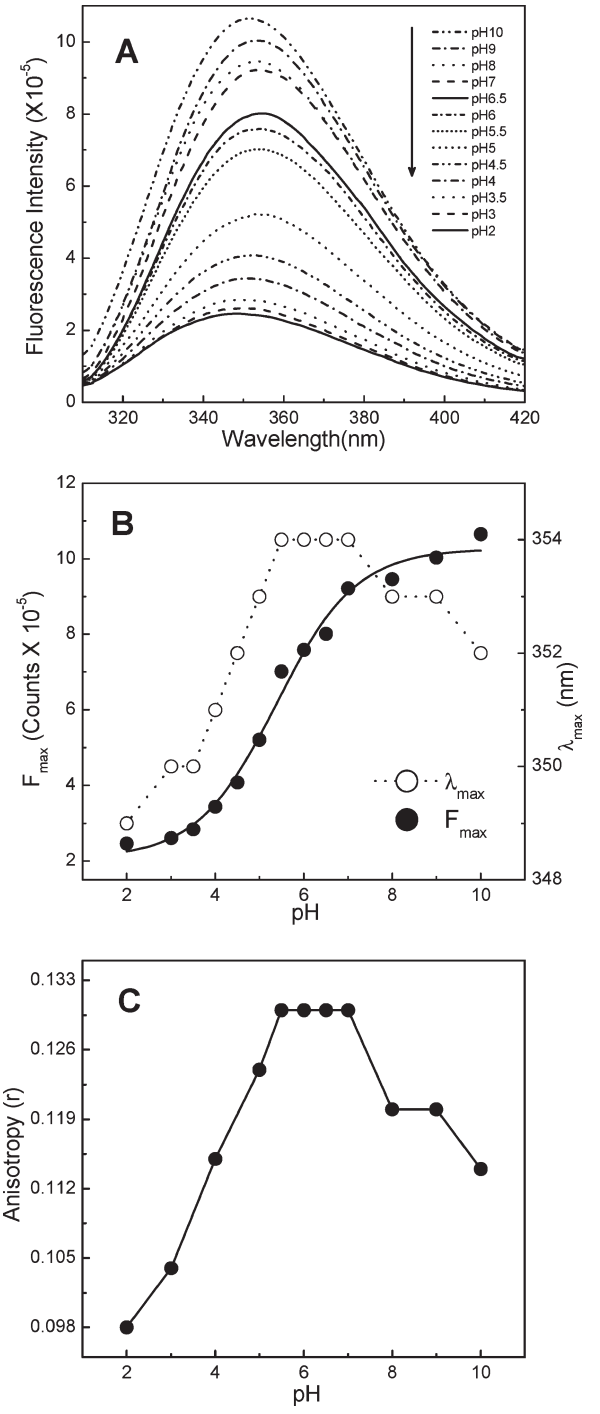

Figure 2. Effect of pH on the intrinsic tryptophan fluorescence of HET-C2. (A) Emission spectra of HET-C2 acquired at the indicated pH values. (B) Fluorescence emission intensity maxima and wavelength maxima (λ_{max}) plotted as a function of pH. (C) Fluorescence anisotropy values of HET-C2 at various pH values. The protein concentration was 1 μM. Fluorescence excitation occurred at 295 nm, and emission measurements were performed as detailed in Experimental Procedures.

in anisotropy are observed at pH 5, 8, and 9; slightly larger decreases occur at pH 4 and 10, and the most pronounced decreases are observed at pH 3 and 2. Because diminished anisotropy indicates an increase in the level of motion of the fluorophore, we concluded that low pH is particularly effective at inducing

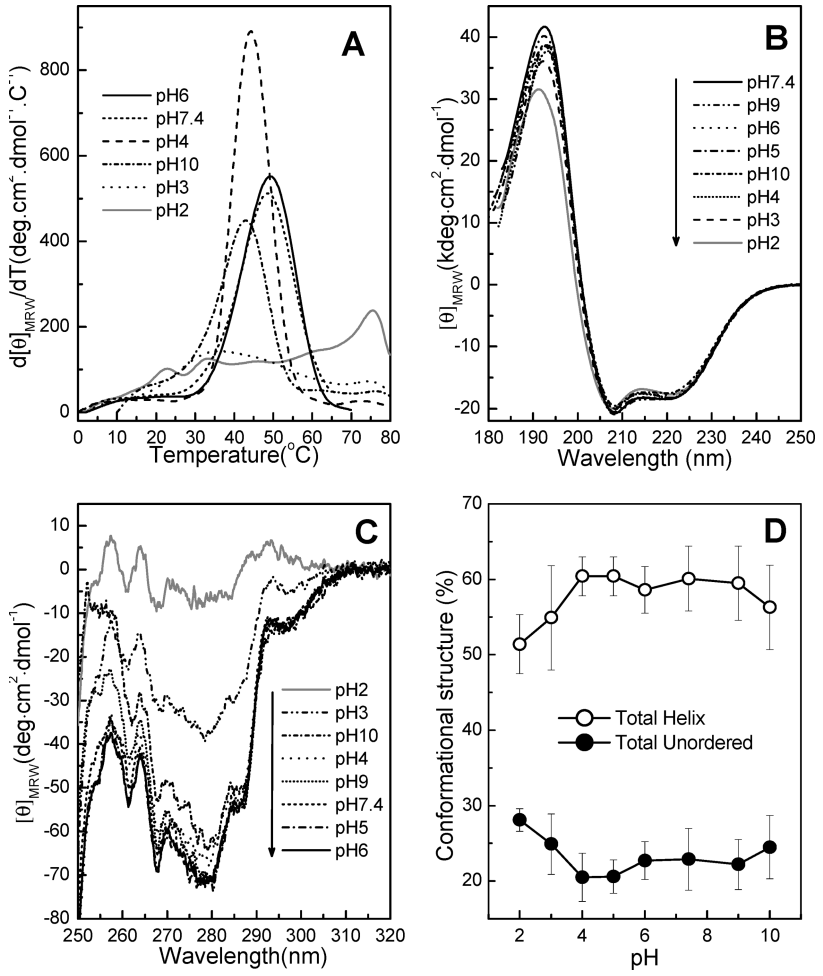

Figure 3. pH-induced conformational changes of HET-C2 at different pH values. Far-UV and near-UV CD spectra of 50 μM HET-C2 were recorded at 10 °C using a J-810 spectropolarimeter as detailed in Experimental Procedures. (A) Temperature dependence of molar ellipticity at 222 nm (derivative plot). Unfolding of HET-C2 is shifted to a lower temperature at pH 3, and unfolding cooperativity is completely lacking at pH 2. (B) Far-UV CD spectra at different pH values presented in units of molar ellipticity per residue. The negative bands at ~208 nm and positive bands at ~192 nm are characteristic of high helical content, with large negative n$-\pi^*$ transitions at 222 nm and $\pi-\pi^*$ transitions split into two transitions because of exciton coupling. HET-C2 secondary structure is nearly identical at all pH values tested. (C) Near-UV CD spectra. The strong signal response from Tyr and Trp in HET-C2 at moderate pH is somewhat disrupted at pH 3 and is almost completely lost at pH 2, consistent with a diminished level of tertiary structure. (D) Change in HET-C2 secondary structure induced by pH. The plotted values illustrate calculations of HET-C2 secondary structure, presented as part of Table S1 of the Supporting Information and obtained from the far-UV CD spectra.

HET-C2 unfolding. Altogether, the fluorescence data suggest that HET-C2 is relatively stable over a wide pH range (e.g., pH 5−9) but becomes destabilized under more extreme pH conditions (pH ≤4 or ≥10).

To gain additional insights into the conformational stability of HET-C2 at various pH values, we used far-UV CD spectroscopy to monitor the first derivative of the CD signal at 222 nm as a function of temperature.[37] The choice of wavelength was dictated by the well-established property of α-helical proteins having a strong CD signal at 222 nm that dramatically decreases in intensity upon unfolding. The heat-induced denaturation profiles in Figure 3A show that HET-C2 undergoes highly cooperative unfolding at pH 7.4 between 25 and 55 °C, with a transition midpoint of ~49 °C. The relatively low temperature midpoint for unfolding is consistent with a lack of stabilization by intramolecular disulfides. At pH 6, the thermal unfolding profile of HET-C2 remained nearly unaltered. At pH 10, the transition temperature midpoint decreased to 44 °C and the unfolding cooperativity decreased, consistent with moderate destabilization of HET-C2. Similar destabilization was indicated at pH 4 by the 43 °C midpoint of the unfolding transition, but there was significant enhancement in the unfolding cooperativity. At pH 3, the unfolding transition temperature midpoint was greatly decreased (T_m ~ 36 °C) and the unfolding transition was extremely broad, occurring over the range of 15−68 °C (Figure 3A). A lower-magnitude transition peak also became evident near 75 °C. At pH 2, the 75 °C transition peak was significantly enhanced while only two minor peaks (~23 and ~34 °C) were evident at lower temperatures, indicating a highly unfolded structure. The heat-induced unfolding transitions of HET-C2 were found to be ~80% reversible at pH 2 and 3 but were only 30% reversible at pH 7.4, upon heating 20−25 °C above the midpoint of the unfolding transition temperature. This finding is consistent with diminished HET-C2 solubility near its isoelectric point, which is estimated to be 6.81 from amino acid composition. Inclusion of dithiothreitol did not improve

dx.doi.org/10.1021/bi200382c |*Biochemistry* 2011, 50, 5163–5171

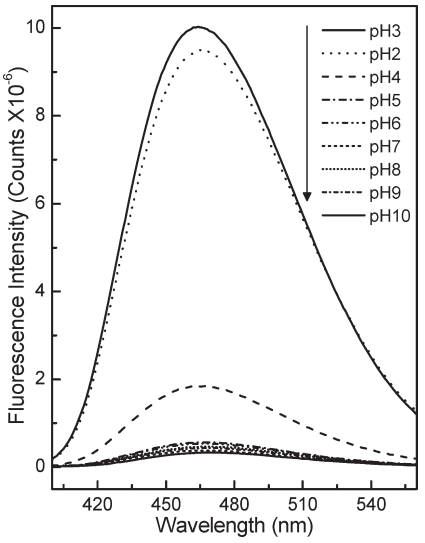

Figure 4. ANS fluorescence at different pH values. HET-C2 (2 μM) was incubated with ANS (10 μM) for 10 min at the indicated pH values, and the fluorescence spectra were recorded. Samples were excited at 375 nm, and emission was measured from 400 to 560 nm.

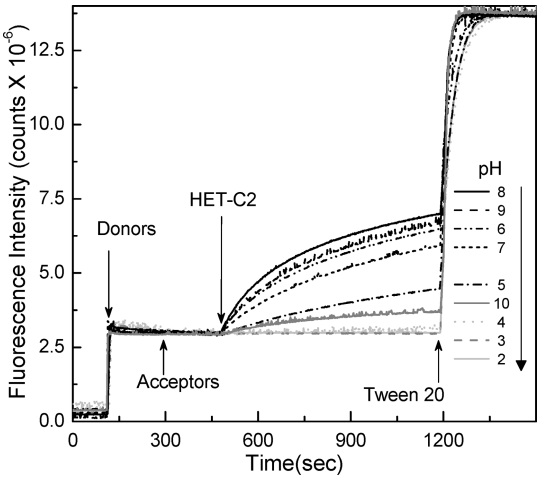

Figure 5. pH-induced change in the glycolipid transfer activity of HET-C2. Förster energy transfer involving fluorescently labeled glycolipid (AV-GalCer) and phospholipid (Perylenoyl-PC) was used to assess glycolipid intervesicular transfer by HET-C2. The stock protein at pH 8 was diluted ~10-fold into buffer of the specified pH and incubated at room temperature for 10 min. Assays were initiated by ~1000-fold dilution of HET-C2 at the indicated pH. AV-GalCer was excited at 370 nm, and emission was monitored at 425 nm. Additional details are provided in Experimental Procedures.

reversibility at neutral pH for GLTP, which responds similarly at low and neutral pH (R. K. Kamlekar, R. Kenoth, and R. E. Brown, unpublished observation). Thus, the thermodynamic parameters attributable to the HET-C2 unfolding transition could not be reliably ascertained at physiological pH.

Does Extreme pH Induce a Molten Globule-like State for HET-C2? Partial unfolding to the molten globule (MG) state is known to occur for many proteins at extreme pH values and has been especially well-studied at low pH.[38,39] To determine whether HET-C2 could undergo a transition to a MG-like state at low or high pH, secondary and tertiary structure was analyzed by CD spectroscopy. Previously, we showed that the secondary structure of HET-C2 at pH 7.4 is dominated by high helical content, i.e., 56.6% helix, 8.8% β-structure, 12.1% β-turns, and 24.1% random, as assessed by far-UV CD.[18] Figure 3B shows far-UV CD spectra recorded at various pH values between 2 and 10. The helical content of HET-C2 remains mostly unaltered over the entire pH range, except for minor changes observed at pH 2. Figure 3D illustrates the stability of HET-C2 helical content and the increase in the level of unordered structure induced by low pH. The data are based on secondary structural calculations (Table S1 of the Supporting Information) derived by CDPro analysis from the far-UV CD spectra.[18,25]

Near-UV CD spectra (Figure 3C), which assess tertiary structure, showed significant environmentally induced optical activity arising from the four Tyr, two Trp, and 12 Phe residues of HET-C2 in between pH 5 and 9. Signals in the 270−290 nm region typically originate from Tyr and those in the 280−300 nm region from Trp, and those in the 250−270 nm region generally are attributed to Phe.[40] In HET-C2, the peak signals at ~255, ~262, and ~277 nm likely belong to the 12 Phe residues, whereas the prominent negative signal near 280 nm along with the shoulder peaks at 287 and 293 nm could originate from Tyr and/or Trp. In any case, the near-UV signal response shows little variation between pH 4 and 9. At a more basic pH (pH 10), only marginally decreased signal intensity is evident in the spectra. In contrast, at pH 3, pronounced change occurs in the near-UV CD signal, suggesting a considerable loss of tertiary folding, while nearly complete loss of tertiary folding is evident at pH 2. Notably, residual signals near 255 and 262 nm, originating from the protein interior core Phe residues, persist at extreme pH. Together, the large reduction in tertiary structure content while maintaining secondary structure and the dramatic loss of thermally induced unfolding cooperativity at pH <4 provide strong evidence of HET-C2 undergoing a transition to a molten globule-like state at low pH.

HET-C2 Unfolding Assessed by ANS Fluorescence Analysis. Changes in ANS fluorescence often are used to monitor formation of folding intermediates during protein unfolding and refolding.[28,41,42] The presence of large solvent-exposed hydrophobic patches is a general property of a partially folded protein. Interaction of ANS with exposed hydrophobic sites on a protein is accompanied by a considerable increase in dye fluorescence intensity and a substantially blue-shifted emission maximum.[41−43] Accordingly, we used ANS fluorescence to study pH-induced conformational changes in HET-C2. Figure 4 shows that ANS emission intensity and λ_{max} values remain nearly unchanged in the presence of HET-C2 from pH 5 to 9. At pH 4, the intensity is slightly elevated. However, at pH 2 and 3, dramatic increases in intensity are observed along with substantial λ_{max} blue shifting, consistent with the appearance of solvent-exposed hydrophobic surfaces. The findings support the CD data showing that low pH transforms HET-C2 to a partially folded intermediate state with molten globule-like properties.

Is Glycolipid Transfer Activity by HET-C2 Helped or Hindered by the pH-Induced Molten Globule-like State? Figure 5 shows how pH affects the glycolipid transfer activity of HET-C2. After preincubation for 10 min at the indicated pH, glycolipid transfer activity was monitored using a well-established Förster resonance energy transfer (FRET) assay that allows real-time kinetic monitoring of fluorescent glycolipid transfer between membranes.[17] Maximal transfer activity was found between pH 6 and 9 (Table 1). Activity was strongly diminished

Table 1. Glycolipid Transfer Activity (initial transfer rate) by HET-C2 as a Function of pH

pH	initial transfer rate of AV-GalCer (pmol/min)[a]	pH	initial transfer rate of AV-GalCer (pmol/min)[a]
2	0.75 ± 0.39	7	16.39 ± 1.46
3	0.25 ± 0.25	8	33.70 ± 0.70
4	1.30 ± 0.08	9	27.79 ± 1.45
5	7.78 ± 0.35	10	3.46 ± 1.04
6	22.07 ± 0.25		

[a] Determined from Förster resonance energy transfer data shown in Figure 5.

(~90%) at pH 10 and ~75% diminished at pH 5. A more acidic pH (e.g., pH 4) resulted in an almost complete loss of activity. At pH 3 or 2, glycolipid transfer by HET-C2 ceased. Having membrane vesicles present during HET-C2 incubation at the indicated pH (prior to assay initiation) did not change the outcome. These findings suggest that formation of an acid-induced, molten globule-like state strongly inhibits the ability of HET-C2 to transfer glycolipid between membranes.

DISCUSSION

This study provides fundamental insights into the stability and folding of HET-C2, a fungal GLTP-like protein with a core architecture that strongly resembles the human GLTP fold. HET-C2 contains an α-helically dominated, two-layer sandwich topology characteristic of the GLTP fold in which helices α1, α2, α6, and α7 make up one layer and helices α3−α5 and α8 helices make up the other layer.[18] HET-C2 contains two Cys residues, Cys^{118} in helix 4 and Cys^{162} in the α6−α7 loop, that are too far apart (15.6 Å) to stabilize conformation via disulfide bridging (Figure S2A of the Supporting Information). An important consequence is moderate temperature stability at neutral pH with an unfolding transition temperature midpoint of ~49 °C.[18] The 4−5 °C lower unfolding transition temperature midpoint of HET-C2 compared to that of human GLTP could reflect adaptation for growth conditions typical for *P. anserina*, a saprophytic fungus inhabiting the dung of herbivores. In any case, the lack of Cys residue conservation (Figure S2 of the Supporting Information) and of intramolecular disulfide bridging in HET-C2 and GLTP clearly distinguishes the GLTP fold from other lipid binding/transfer protein folds that also are dominated by α-helices, i.e., saposins and nonspecific plant lipid transfer proteins (nsLTP folds).[22] The saposin motif is characterized by a set of five helices, sometimes arranged in two layers, but always connected by a conserved pattern of three intramolecular disulfide bonds that impart heat stability.[44−49] In nsLTP folds, the core tertiary superstructure consists of multiple helices, bundled to form a large central, tunnel-like hydrophobic cavity.[50−55] The spatial arrangement of eight cysteines, interspersed to form four interhelical disulfide bridges, stabilizes the bundlelike structure and is thought to be important for maintaining tertiary structure when the large central hydrophobic tunnel is devoid of lipid ligand.[52,55] A consequence of the multiple-disulfide bridging is remarkable heat stability with unfolding transition temperatures in the 90−100 °C range.[50]

What Fluorescence and CD Reveal about HET-C2 Stability and Functionality. Despite the moderate temperature stability, the HET-C2 GLTP fold remains relatively stable over a wide pH range extending from 5 to 10, as revealed by intrinsic signal changes obtained from fluorescence (e.g., Trp) and CD spectroscopic analyses. The indole rings for both Trp residues in HET-C2 are solvent-exposed (Figure S3 of the Supporting Information), resulting in a more highly red-shifted emission λ_{max} (~355 nm) compared to that of GLTP ($\lambda_{max} \approx 348$ nm), in which the solvent accessibility of one of three Trp residues is relatively restricted. The responsiveness of HET-C2 Trp emission to the change in pH appears to reflect altered interactions with neighboring His residues. In the case of Trp^{208}, the indole ring stacks against the His^{101} imidazole ring (~3.2 Å). Water-bridged hydrogen bonding of His^{101} with Glu^{105} helps keep the imidazole ring favorably aligned for stacking against the Trp^{208} indole ring. The His^{101}−Trp^{208} π-stack and associated hydrogen bonding interactions have the net effect of altering the conformation of the C-terminal region of HET-C2 compared to that of GLTP.[18] With Trp^{109}, interaction with His^{146} is indirect and occurs by networking through Arg^{112} as shown in Figure 1 and detailed earlier. Because of the involvement of the His residues, which change their ionization state at a relatively moderate pH,[56] the responsiveness of the two Trp residues is not surprising. Quenching by increased levels of protonated histidine probably contributes to the diminished Trp emission intensity accompanying the stepwise pH decreases between 6 and 4. Considering the surface location of the His^{101}−Trp^{208} stack and the aqueous accessibility of the Trp^{109}−Arg^{112}−His^{146} network, the net pK value of ~5.5 that can be approximated from the Trp fluorescence data is reasonable.[56,57] It is noteworthy that other residues known to quench Trp emission, i.e., Cys and Tyr, are not sufficiently close to be effective quenchers.[58] Both Cys residues (pK_a ~ 8.6) are >17 Å from either Trp residue. All four Tyr residues (pK_a ~ 9.8) are >20 Å distant except for Tyr^{139}, which is 8−10 Å from Trp^{109}. The closest Lys residues (Lys^{73}, Lys^{152}, and Lys^{207}) (pK_a ~ 10.4) are 8−11 Å distant, weakening their ability to quench by H^+ transfer.[58] In contrast, the proximity of His and the established ability of protonated histidine to quench Trp fluorescence are consistent with a major role for His in the regulation of HET-C2 Trp emission intensity.[57−62]

Although quenching of Trp by protonated His is likely to increase over the pH range from 6 to 4, the diminished Trp anisotropy also suggests an accompanying Trp conformational change. The local nature of the conformational change is supported by the nearly unaltered far-UV and near-UV CD spectra at pH 4, 5, 6, and 7.4 as well as by only slightly altered thermal midpoints of unfolding. What is noteworthy with respect to HET-C2 GLTP fold functionality is the robust glycolipid transfer activity over the pH range of 6−9, but the precipitous drop in glycolipid transfer activity at moderately acidic pH values of 5 and 4, when native global folding still remains largely unaltered. Thus, the local interactions between Trp and His appear to play a crucial regulatory role in controlling the glycolipid transfer activity of HET-C2.

At pH <4, the fluorescence data for Trp and ANS and the near-UV CD spectra indicate global alterations in HET-C2 conformation that result in a loss of glycolipid transfer activity. The low-pH-induced changes are likely to alter the two interchain cation−π interactions involving His^{101} and His^{146} and disrupt one or more of the numerous salt bridges involving Asp and Glu residues (pK_a = 3.9 and 4.3, respectively) (Table 2). Among the salt bridges, two are complex or networked bridges (Glu^{46}−Arg^{75}−Glu^{72} and Asp^{90}−Arg^{93}−Glu^{205}) along with a half-dozen single bridges that are interchain rather than intrahelical in nature.[63] While the effect of pH change on GLTP has been

Table 2. Inter-Residue Interactions of the HET-C2 GLTP Fold[a]

salt bridge (<4.0 Å)	nature of the interaction
E^{17}–K^{178} (~3.6 Å)	$\eta1$–α8, interchain
*E^{46}–R^{75} (~2.8 Å)	α1–α2, interchain
D^{53}–K^{64} (~3.6 Å)	α1–α2, interchain
*E^{72}–R^{75} (~2.8 Å)	α2–α2, intrahelix
E^{84}–R^{77} (~3.5 Å)	α2-α3 coil–α2, interchain
*D^{90}–R^{93} (~2.8 Å)	α3–α3, intrahelix
*E^{205}–R^{93} (~2.9 Å)	$\eta6$–α3, interchain
E^{105}–H^{101} (~3.7 Å)	α4–α3-α4 coil, interchain
E^{115}–K^{198} (~3.4 Å)	α4–α8, interchain
K^{123}–E^{129} (~3.9 Å)	α4–α4-α5 coil, interchain
D^{133}–R^{136} (~3.1 Å)	α5–α5, intrahelix
cation–π (<5.0 Å)	
W^{96}–R^{112} (~3.4 Å)	α4–α4, intrahelix
W^{208}–H^{101} (~3.5 Å)	COOH–α4-α5 coil, interchain
F^{149}–K^{152} (~5.1 Å)	α6–α6, intrahelix
H^{146}–R^{112} (~3.4 Å)	$\eta5$–α4, interchain
H_2O-bridging (<3.0 Å)	
E^{105}–H_2O–H^{101} (2.6–2.6 Å)	α4–α3-α4 coil, interchain
H^{147}–H_2O–D^{66} (2.8–2.5 Å)	$\eta5$–α2, interchain
E^{105}–H_2O–W^{96} (~2.8–2.4 Å)	α4–α4, intrachain

[a] The distances between residue side chains are derived from our HET-C2 X-ray structure (1.9 Å; Protein Data Bank entry 3kv0),[18] which also identifies residue location within secondary structural elements (see Figure S2 of the Supporting Information, bottom panel). Salt bridges are indicated by oppositely charged residues within 4 Å of each other (e.g., ref 63). Asterisks indicate networked salt bridges involving Arg^{75} and Arg^{93}. The cation–π interaction between Arg^{112} and Trp^{109} is predicted as energetically favored by the on-line CaPTURE program (http://capture.caltech.edu).[35] His^{146} and Arg^{112} π-stacking and pH-dependent cation–π interactions (in bold) are supported by experimental data[57−61] and by computational modeling of His–Arg interactions in peptides.[36]

reported by West et al.,[34] their focus was exclusively on transfer activity over the pH range of 4–10 without accompanying conformational insights.

Functional Consequences of the Low-pH-Induced MG-like State in HET-C2. MG-like states reportedly help many amphitropic peripheral membrane proteins perform their biological functions by promoting association with membranes.[24] Lactalbumin,[8] retinol binding protein,[38] colicin A,[7] diphtheria toxin T-domain,[5] StaR lipid binding domains,[10] and barley nsLTP[12] are a few such proteins. The GLTP fold represents both a novel motif among lipid binding/transfer proteins and a novel membrane interaction motif among amphitropic peripheral proteins that translocate to membranes while carrying out their function.[25] For this reason, the existence and potential role of a MG-like state for the HET-C2 GLTP fold were of interest. Such states typically are characterized by maintenance of or increase in the level of secondary structure, a loss of tertiary structure, and a loss of cooperativity of melting.[1−4] In this respect, it is noteworthy that our CD spectra reveal the maintenance of HET-C2 regular secondary structure and partial loss of tertiary structure at pH 3, in contrast to the complete loss of tertiary structure observed at pH 2. Also, a considerable decrease in the unfolding transition temperature and loss of unfolding cooperativity are observed at pH 3, but complete loss occurs at pH 2. The dramatic enhancement of ANS fluorescence intensity is evident upon binding by HET-C2 at pH 3 and 2. Thus, the experimental data are consistent with the existence of an MG-like state at low pH. However, it is clear from the activity measurements that glycolipid transfer activity by HET-C2 is completely lost at pH 3, indicating that the pH-induced, MG-like state does not promote glycolipid transfer by the HET-C2 GLTP fold.

It is worthwhile to recall that HET-C2 plays important functional roles that may occur in a manner independent of its glycolipid binding/transfer ability. *Het* genes exhibit extensive polymorphism and generally encode proteins carrying a HET domain. In *P. anserina*, the process of protoplasmic incompatibility involves cell destruction that can be triggered by interaction of *het-C* alleles (e.g., *het-c2* encoding GLTP-like HET-C2) and *het-E*, encoding a HET domain and a WD repeat domain involved in recognition.[64] The structural similarity of HET-E and mammalian APAF-1, a protein controlling cytochrome *c*-induced apoptosis, suggests parallels between cell death by incompatibility and programmed cell death mechanisms in higher eukaryotes. It has been proposed that cytochrome *c* binds to APAF-1 in the cytoplasm to form a complex that initiates enzymatic cascades leading to apoptosis. Cytochrome *c* is thought to be released from mitochondria in the MG state during apoptosis. Within this context, the current observation of the transition of HET-C2 to the MG-like state at low pH may be significant. Modifications of the vacuolar compartment are frequently observed during cell death reactions. Vacuole membrane permeabilization or rupture followed by liberation of lytic enzymes and acidification of the cytoplasm is proposed to be involved in cell death by incompatibility in filamentous fungi. In this acidic environment, it is tempting to speculate that HET-C2 may achieve a partially unfolded conformation that is functionally important to the fungal incompatibility cell death response. Clearly, additional cell biological experiments will be needed to further evaluate these ideas.

■ ASSOCIATED CONTENT

Supporting Information. One table summarizing HET-C2 secondary structure, as computed from the far-UV CD spectra and three images of HET-C2 conformation. This material is available free of charge via the Internet at http://pubs.acs.org.

■ AUTHOR INFORMATION

Corresponding Author

*E-mail: D.J.P. pateld@mskcc.org; S.Y.V. venyaminova@hotmail.com; R.E.B. reb@umn.edu.

Author Contributions

¶R.K., R.K.K., and D.K.S. contributed equally to this work.

Funding Sources

We are grateful for financial support by National Institute of General Medical Sciences Grants GM45928 and GM34847, National Cancer Institute Grant CA121493, Spanish Ministerio de Ciencia e Innovacion (MICINN BFU2010-17711), the Russian Foundation for Basic Research (09-04-00313), the Abby Rockefeller Mauzé Trust, and the Dewitt Wallace, Maloris, Mayo, and Hormel Foundations.

■ ACKNOWLEDGMENT

We thank Helen Pike for expressing and purifying the HET-C2 protein and the Resource for Biocomputing, Visualization, and Informatics of the University of California, San Francisco, CA (National Institutes of Health Grant P41 RR-01081), for the use of Chimera.

■ ABBREVIATIONS

HET-C2, heterokaryon incompatibility C2 protein; GLTP, glycolipid transfer protein; MG, molten globule; ANS, 1-anilinonaphthalene-8-sulfonic acid; CD, circular dichroism; FRET, Förster resonance energy transfer; UV, ultraviolet; AV, anthrylvinyl; Per, 3-perylenoyl; PC, 1,2-acyl-*sn*-glycero-3-phosphocholine; POPC, 1-palmitoyl-2-oleoyl-*sn*-glycero-3-phosphocholine.

■ REFERENCES

(1) Dolgikh, D. A., Gilmanshin, R. I., Brazhnikov, E. V., Bychkova, V. E., Semisotnov, G. V., Venyaminov, S. Y., and Ptitsyn, O. B. (1981) α-Lactalbumin: Compact state with fluctuating tertiary structure. *FEBS Lett. 136*, 311–315.

(2) Dobson, C. M. (1992) Unfolded proteins, compact states and molten globules. *Curr. Opin. Struct. Biol. 2*, 6–12.

(3) Dobson, C. M. (1994) Protein folding: Solid evidence for molten globules. *Curr. Biol. 4*, 636–640.

(4) Ptitsyn, O. B., Bychkova, V. E., and Uversky, V. N. (1995) Kinetic and equilibrium folding intermediates. *Philos. Trans. R. Soc. London, Ser. B 348*, 35–41.

(5) Ren, J., Kachel, K., Kim, H., Malenbaum, S. E., Collier, R. J., and London, E. (1999) Interaction of diphtheria toxin T domain with molten globule-like proteins and its implications for translocation. *Science 284*, 955–957.

(6) Bychkova, V. E., Pain, R. H., and Ptitsyn, O. B. (1988) The 'molten globule' state is involved in the translocation of proteins across membranes? *FEBS Lett 238*, 231–234.

(7) van der Goot, F. G., Gonzalez-Manas, J. M., Lakey, J. H., and Pattus, F. (1991) A 'molten-globule' membrane-insertion intermediate of the pore-forming domain of colicin A. *Nature 354*, 408–410.

(8) Bañuelos, S., and Muga, A. (1995) Binding of molten globule-like conformations to lipid bilayers. *J. Biol. Chem. 270*, 29910–29915.

(9) Bose, H. S., Whittal, R. M., Baldwin, M. A., and Miller, W. L. (1999) The active form of the steroidogenic acute regulatory protein, StAR, appears to be a molten globule. *Proc. Natl. Acad. Sci. U.S.A. 96*, 7250–7255.

(10) Song, M., Shao, H., Mujeeb, A., James, T. L., and Miller, W. L. (2001) Molten-globule structure and membrane binding of the N-terminal protease-resistant domain (63−193) of the steroidogenic acute regulatory protein (StAR). *Biochem. J. 356*, 151–158.

(11) Greene, L. H., Wijesinha-Bettoni, R., and Redfield, C. (2006) Characterization of the molten globule of human serum retinol-binding protein using NMR spectroscopy. *Biochemistry 45*, 9475–9484.

(12) Mills, E. N. C., Gao, C., Wilde, P. J., Rigby, N. M., Wijesinha-Bettoni, R., Johnson, V. E., Smith, L. J., and Mackie, A. R. (2009) Partially-folded forms of barley lipid transfer protein are more surface active. *Biochemistry 48*, 12081–12088.

(13) Saupe, S. J. (2000) Molecular genetics of heterokaryon incompatibility in filamentous Ascomycetes. *Microbiol. Mol. Biol. Rev. 64*, 489–502.

(14) Glass, N. L., and Kaneko, I. (2003) Fatal attraction: Nonself recognition and heterokaryon incompatibility in filamentous fungi. *Eukaryotic Cell 2*, 1–8.

(15) Federova, N. D., Badger, J. H., Robson, G. D., Wortman, J. R., and Nierman, W. C. (2005) Comparative analysis of programmed cell death pathways in filamentous fungi. *BMC Genomics 6*, 177.

(16) Paoletti, M., Saupe, S. J., and Clave, C. (2007) Genesis of a fungal non-self recognition repertoire. *PLoS One 2*, e283.

(17) Mattjus, P., Turcq, B., Pike, H. M., Molotkovsky, J. G., and Brown, R. E. (2003) Glycolipid intermembrane transfer is accelerated by HET-C2, a filamentous fungus gene product involved in the cell-cell incompatibility response. *Biochemistry 42*, 535–542.

(18) Kenoth, R., Simanshu, D. K., Kamlekar, R. K., Pike, H. M., Molotkovsky, J. G., Benson, L. M., Bergen, H. R., III, Prendergast, F. G., Malinina, L., Venyaminov, S. Y., Patel, D. J., and Brown, R. E. (2010) Structural determination and tryptophan fluorescence of heterokaryon incompatibility C2 protein (HET-C2), a fungal glycolipid transfer protein (GLTP), provide novel insights into glycolipid specificity and membrane interaction by the GLTP fold. *J. Biol. Chem. 285*, 13066–13078.

(19) Malinina, L., Malakhova, M. L., Teplov, A., Brown, R. E., and Patel, D. J. (2004) Structural basis for glycosphingolipid transfer specificity. *Nature 430*, 1048–1053.

(20) Malinina, L., Malakhova, M. L., Kanack, A. T., Lu, M., Abagyan, R., Brown, R. E., and Patel, D. J. (2006) The liganding of glycolipid transfer protein is controlled by glycolipid acyl structure. *PLoS Biol. 4*, e362.

(21) Airenne, T. T., Kidron, H., Nymalm, Y., Nylund, M., West, G. P., Mattjus, P., and Salminen, T. A. (2006) Structural evidence for adaptive ligand binding of glycolipid transfer protein. *J. Mol. Biol. 355*, 224–236.

(22) Brown, R. E., and Mattjus, P. (2007) Glycolipid transfer proteins. *Biochim. Biophys. Acta 1771*, 746–760.

(23) Johnson, J. E., and Cornell, R. B. (1999) Amphitropic proteins: Regulation by reversible membrane interactions. *Mol. Membr. Biol. 16*, 217–235.

(24) Halskau, O., Arturo Muga, A., and Martínez, A. (2009) Linking new paradigms in protein chemistry to reversible membrane-protein interactions. *Curr. Protein Pept. Sci. 10*, 339–359.

(25) Kamlekar, R.-K., Gao, Y., Kenoth, R., Pike, H. M., Molotkovsky, J. G., Prendergast, F. G., Malinina, L., Patel, D. J., Wessels, W., Venyaminov, S. Y., and Brown, R. E. (2010) Human GLTP: Three distinct functions for the three tryptophans in a novel peripheral amphitropic fold. *Biophys. J. 90*, 2626–2635.

(26) Nylund, M., and Mattjus, P. (2005) Protein mediated glycolipid transfer is inhibited FROM sphingomyelin membranes but enhanced TO sphingomyelin containing raft like membranes. *Biochim. Biophys. Acta 1669*, 87–94.

(27) Malakhova, M. L., Malinina, L., Pike, H. M., Kanack, A. T., Patel, D. J., and Brown, R. E. (2005) Point mutational analysis of the liganding site in human glycolipid transfer protein. Functionality of the complex. *J. Biol. Chem. 280*, 26312–26320.

(28) Li, X.-M., Malakhova, M. L., Lin, X., Pike, H. M., Chung, T., Molotkovsky, J. G., and Brown, R. E. (2004) Human glycolipid transfer protein: Probing conformation using fluorescence spectroscopy. *Biochemistry 43*, 10285–10294.

(29) Zhai, X., Malakhova, M. L., Pike, H. M., Benson, L. M., Bergen, H. R., III, Sugar, I. P., Malinina, L., Patel, D. J., and Brown, R. E. (2009) Glycolipid acquisition by human glycolipid transfer protein dramatically alters intrinsic tryptophan fluorescence: Insights into glycolipid liganding affinity. *J. Biol. Chem. 284*, 13620–13628.

(30) Mihaly, E. J. (1968) Numerical values of the absorbances of the aromatic amino acids in acid, neutral and alkaline solutions. *Chem. Eng. Data 13*, 179–182.

(31) Gill, S. C., and von Hippel, P. H. (1989) Calculation of protein extinction coefficients from amino acid sequence data. *Anal. Biochem. 182*, 319–326.

(32) Mach, H., Middaugh, C. R., and Lewis, R. V. (1992) Statistical determination of the average values of the extinction coefficients of tryptophan and tyrosine in native proteins. *Anal. Biochem. 200*, 74–80.

(33) Pace, C. N., Vajdos, F., Fee, L., Grimsley, G., and Gray, T. (1995) How to measure and predict the molar absorption coefficient of a protein. *Protein Sci. 4*, 2411–2423.

(34) West, G., Nylund, M., Slotte, J. P., and Mattjus, P. (2006) Membrane interaction and activity of the glycolipid transfer protein. *Biochim. Biophys. Acta 1758*, 1732–1742.

(35) Gallivan, J. P., and Dougherty, D. A. (1999) Cation-π interactions in structural biology. *Proc. Natl. Acad. Sci. U.S.A. 96*, 9459–9464.
(36) Heyda, J., Mason, P. E., and Jungwirth, P. (2010) Attractive interactions between side chains of histidine-histidine and histidine-arginine-based cationic dipeptides in water. *J. Phys. Chem. B 114*, 8744–8749.
(37) Kelly, S. M., Jess, T. J., and Price, N. C. (2005) How to study proteins by circular dichroism. *Biochim. Biophys. Acta 1751*, 119–139.
(38) Bychkova, V. E., Berni, R., Rossi, G. L., Kutyshenko, V. P., and Ptitsyn, O. B. (1992) Retinol-binding protein is in the molten globule state at low pH. *Biochemistry 31*, 7566–7571.
(39) Redfield, C., Smith, R. A. G., and Dobson, C. M. (1994) Structural characterization of a highly structured 'molten globule' at low pH. *Nat. Struct. Biol. 1*, 23–29.
(40) Greenfield, N. J. (2006) Using circular dichroism collected as a function of temperature to determine the thermodynamics of protein unfolding and binding interactions. *Nat. Protoc. 1*, 2527–2535.
(41) Semisotnov, G. V., Rodionova, N. A., Razgulyaev, O. I., Uversky, V. N., Cripaś, A. F., and Gilmanshin, R. I. (1991) Study of the "Molten Globule" intermediate state in protein folding by a hydrophobic fluorescent probe. *Biopolymers 31*, 119–128.
(42) Rosen, C. G., and Weber, G. (1969) Dimer formation from 1-anilino-8-naphthalenesulfonate catalyzed by bovine serum albumin. Fluorescent molecule with exceptional binding properties. *Biochemistry 8*, 3915–3920.
(43) Hawe, A., Sutter, M., and Jiskoot, W. (2008) Extrinsic fluorescent dyes as tools for protein characterization. *Pharm. Res. 25*, 1487–1499.
(44) Kishimoto, Y., Hiraiwa, M., and O'Brien, J. S. (1992) Saposins: Structure, function, distribution, and molecular genetics. *J. Lipid Res. 33*, 1255–1267.
(45) Liepinsh, E., Andersson, M., Ruysschaert, J.-M., and Otting, G. (1997) Saposin fold revealed by the NMR structure of NK-lysin. *Nat. Struct. Biol. 4*, 793–795.
(46) Ahn, V. E., Faull, K. F., Whitelegge, J. P., Fluharty, A. L., and Privé, G. G. (2003) Crystal structure of saposin B reveals a dimeric shell for lipid binding. *Proc. Natl. Acad. Sci. U.S.A. 100*, 38–43.
(47) Ahn, V. E., Leyko, P., Alattia, J.-R., Chen, L., and Privé, G. G. (2006) Crystal structures of saposins A and C. *Protein Sci. 15*, 1849–1857.
(48) John, M., Wendeler, M., Heller, M., Sandhoff, K., and Kessler, H. (2006) Characterization of human saposins by NMR spectroscopy. *Biochemistry 45*, 5206–5216.
(49) Popovic, K., and Privé, G. G. (2008) Structures of the human ceramide activator protein saposin D. *Acta Crystallogr. D64*, 589–594.
(50) Samuel, D., Liu, Y.-J., Cheng, C.-S., and Lyu, P.-C. (2002) Solution structure of plant nonspecific lipid transfer protein-2 from rice (*Oryza sativa*). *J. Biol. Chem. 277*, 35267–35273.
(51) Pons, J.-L., de Lamotte, F., Gautier, M.-F., and Delsuc, M.-A. (2003) Refined solution structure of a liganded type 2 wheat nonspecific lipid transfer protein. *J. Biol. Chem. 278*, 14249–14256.
(52) José-Estanyol, M., Gomis-Rüth, F. X., and Puigdomènech, P. (2004) The eight-cysteine motif, a versatile structure in plant proteins. *Plant Physiol. Biochem. 42*, 355–365.
(53) Hoh, F., Pons, J.-L., Gautier, M.-F., de Lamotte, F., and Dumas, C. (2005) Structure of a liganded type 2 non-specific lipid transfer protein from wheat and the molecular basis of lipid binding. *Acta Crystallogr. D61*, 397–406.
(54) de Oliveira Carvalho, A., and Gomes, V. M. (2007) Role of plant lipid transfer proteins in plant cell physiology: A concise review. *Peptides 28*, 1144–1153.
(55) Yeats, T. H., and Rose, J. K. C. (2008) The biochemistry and biology of extracellular plant lipid-transfer proteins (LTPs). *Protein Sci. 17*, 191–198.
(56) Grimsley, G. R., Scholtz, J. M., and Pace, C. N. (2009) A summary of the measured pK values of the ionizable groups in folded proteins. *Protein Sci. 18*, 247–251.
(57) Okada, A., Miura, T., and Takeuchi, H. (2001) Protonation of histidine and histidine-tryptophan interaction in the activation of the M2 ion channel from influenza A virus. *Biochemistry 40*, 6053–6060.
(58) Chen, Y., and Barkley, M. D. (1998) Toward understanding tryptophan fluorescence in proteins. *Biochemistry 37*, 9976–9982.
(59) Shinitzky, M., and Goldman, R. (1967) Fluorometric detection of histidine-tryptophan complexes in peptides and proteins. *Eur. J. Biochem. 3*, 139–144.
(60) Vos, R., and Engelborghs, Y. (1994) A fluorescence study of tryptophan-histidine interactions in the peptide anantin and in solution. *Photochem. Photobiol. 60*, 24–32.
(61) Otomo, K., Toyama, A., Miura, T., and Takeuchi, H. (2009) Interactions between histidine and tryptophan residues in the BM2 proton channel from influenza B virus. *J. Biochem. 145*, 543–554.
(62) Smirnova, I., Kasho, V., Sugihara, J., and Kaback, H. R. (2009) Probing of the rates of alternating access in LacY with Trp fluorescence. *Proc. Natl. Acad. Sci. U.S.A. 106*, 21561–21566.
(63) Donald, J. E., Kulp, D. W., and DeGrado, W. F. (2011) Salt bridges: Geometrically specific, designable interactions. *Proteins 79*, 898–915.
(64) Paoletti, M., and Clave, C. (2007) The fungus-specific HET domain mediates programmed cell death in *Podospora anserine*. *Eukaryotic Cell 6*, 2001–2008.